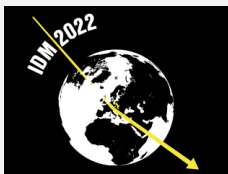# Dark Matter phenomenology in 2HDMS

Gudrid Moortgat-Pick[1,2]⋆, Juhi Dutta[1], Cheng Li[2],
Merle Schreiber[1,2], Sheikh F. Tabira[1] and Julia Ziegler[1]

1 II. Inst. of Theo. Phys., University of Hamburg,
Luruper Chaussee 149, 22761 Hamburg, Germany
2 Deutsches Elektronen-Synchrotron DESY,
Notkestr. 85, 22607 Hamburg, Germany

⋆ gudrid.moortgat-pick@desy.de

Abstract

The constituents of dark matter are still an unresolved puzzle. Several Beyond Standard Model (BSM) Physics offer suitable candidates. In this study here we consider the Two Higgs Doublet model augmented with a complex scalar singlet (2HDMS) and focus on the dark matter phenomenology of 2HDMS with the complex scalar singlet as the dark matter candidate. The parameter space allowed from existing experimental constraints from dark matter, flavour physics and collider searches has been studied. The discovery potential for such a 2HDMS at HL-LHC and at future e^+e^- colliders has been worked out.

Contents

1 Introduction

Dark Matter (DM) remains an unsolved puzzle at the interface between particle physics and cosmology, only 4-5% of the Universe are composed by 'known' matter components, but about 25% is built of dark matter. Since the Standard Model (SM) does not accommodate a suitable DM candidate, several Beyond Standard Model (BSM) extensions have been proposed to accommodate DM candidates ranging from scalar, fermion to vector candidates and with mass scales from below eV up to TeV particles. We concentrate in this contribution on thermal weakly interacting massive particles (WIMP) that is expected in the mass range of GeV up to TeV, accessible at future collider experiments at the LHC and a high-energy e^+e^- linear collider (ILC, CLIC).

Among popular BSM candidates are models with an extended Higgs sector such as the Two Higgs Doublet model (2HDM) [1], providing a dark matter candidate within the Inert Doublet model [1]. Alternate models are such multi-Higgs models but extended via real or complex singlet scalars serving as dark matter candidates. Such extensions involving real scalar singlets have been extensively studied [2–4] while complex scalar extensions to the 2HDM have also been recently studied in the context of modified Higgs sectors [5]. Such models have also the potential to explain the matter-antimatter asymmetry and to accommodate both inflation as well as gravitational waves phenomenology [6, 7]. The parameter space of such extensions of the SM [8] gets strong constraints from direct searches for DM as well as from precision measurements of the 125 GeV SM-like Higgs boson and in particular from limits of both its visible as well as invisible branching ratios [9].

2 Extended two Higgs doublet model

2.1 Symmetries

We consider the CP-conserving softly broken Type II Two Higgs Doublet model augmented with a complex scalar singlet (2HDMS) [5] consistent with flavour changing neutral currents (FCNCs) at tree-level. It allows for the presence of the mixing term between the two Higgs doublets, Φ_1 and Φ_2, i.e., m_{12}^2, while the explicit Z_2 breaking terms are absent. The complex scalar singlet S is stabilised by a Z_2' symmetry such that S is odd under Z_2' while the SM fields are even under the new Z_2' symmetry. The fields Φ_1 and S are even under Z_2 while Φ_2 is odd under Z_2.

We consider the case where Z_2' remains unbroken both explicitly and dynamically, i.e. the scalar singlet doesn't obtain a vacuum expectation value. Therefore, the scalar potential V with a softly broken Z_2- and a conserved Z_2' symmetry is $V = V_{2HDM} + V_S$, where, the softly broken Z_2-symmetric 2HDM potential is:

$$V_{2HDM} = m_{11}^2 \Phi_1^\dagger \Phi_1 + m_{22}^2 \Phi_2^\dagger \Phi_2 - (m_{12}^2 \Phi_1^\dagger \Phi_2 + h.c) + \frac{\lambda_1}{2}(\Phi_1^\dagger \Phi_1)^2 + \frac{\lambda_2}{2}(\Phi_2^\dagger \Phi_2)^2 \tag{1}$$

$$+ \lambda_3(\Phi_1^\dagger \Phi_1)(\Phi_2^\dagger \Phi_2) + \lambda_4(\Phi_1^\dagger \Phi_2)(\Phi_2^\dagger \Phi_1) + \left[\frac{\lambda_5}{2}(\Phi_1^\dagger \Phi_2)^2 + h.c\right], \tag{2}$$

and the Z_2'-symmetric singlet potential, V_S, is

$$V_S = m_S^2 S^* S + (\tfrac{m_S^{2\prime}}{2} S^2 + h.c) + (\tfrac{\lambda_1''}{24} S^4 + h.c) + (\tfrac{\lambda_2''}{6}(S^2 S^* S) + h.c) + \tfrac{\lambda_3''}{4}(S^* S)^2 \qquad (3)$$

$$+ S^* S[\lambda_1' \Phi_1^\dagger \Phi_1 + \lambda_2' \Phi_2^\dagger \Phi_2] + [S^2(\lambda_4' \Phi_1^\dagger \Phi_1 + \lambda_5' \Phi_2^\dagger \Phi_2) + h.c.]. \qquad (4)$$

The doublet fields have the components $\Phi_1 = (h_1^+, \frac{1}{\sqrt{2}}(v_1 + h_1 + ia_1))^T$, $\Phi_2 = (h_2^+, \frac{1}{\sqrt{2}}(v_2 + h_2 + ia_2))^T$, $S = \frac{1}{\sqrt{2}}(h_s + ia_s)$ and $\tan\beta = \frac{v_2}{v_1}$ is the ratio of the up-type and down-type Higgs doublet *vevs* $v_{1,2}$ (with $v(= v_1^2 + v_2^2) \simeq 246$ GeV. Under the assumption that the complex singlet scalar does not develop a *vev* —for this study imposed—, the Higgs sector, after EWSB, remains the same as in 2HDM, i.e, consisting of two CP-even neutral scalar Higgs particles h, H, a pseudoscalar Higgs A and a pair of charged Higgs particles $H^\pm$ [1]. All Higgs-dark-matter portal couplings are explicitly given in [10].

2.2 Theoretical and phenomenological constraints

The Sylvester's criterion and copositivity [11, 12] has been applied to guarantee bounded-ness from below for the Higgs potential, leading to constraints on all coupling parameters λ_i, $i = 1, \ldots, 5$, λ_j', $j = 1, \ldots, 5$, λ_k'', $k = 1, \ldots, 3$. The mass of the lightest CP-even Higgs particle $m_h = 125$ GeV has been chosen to be in concordance with the measured Higgs state via HiggsSignals [13] and collider constraints from LEP and LHC have been applied for the heavy Higgs states via HiggsBounds [14]. The branching ratio $BR(h \to \chi\chi) < 0,11$ (< 0.19), fulfilling the limits from ATLAS (CMS). Electroweak precision constraints on STU parameters have been taken into account as well as constraints from flavour physics $BR(b \to s\gamma)$, $BR(B_s \to \mu^+\mu^-)$, using SPheno [15]. $\Delta(g_\mu - 2)$. Concerning the dark matter particle, the bounds on the relic density from PLANCK measurements, $\Omega h^2 = 0.119$ [16], as well as constraints from direct detection (XENON-1T [17]) and indirect detection (FERMI-LAT [18]) experiments have been applied using micrOMEGAs [19].

3 Results

3.1 Benchmark points

This model has been implemented using SARAH [20] code implemented into SPheno for the spectrum generation. In order to calculate collider observables the code chain Madgraph [21] -Pythia [22] -Delphes [23] -Madanalysis [24] has been used.

As can be seen from Figs.1a) and b) the mass of the dark matter particle χ as well as the coupling λ_2' get strongest constraints from the direct detection search from XENON-1T: in the shown example where the heavier Higgs particles are about 725 GeV, the mass $m_\chi \sim 338$ GeV. Scanning the available parameter space allowed to specify different benchmark areas, see Table I. BP1 and BP3 are very similar, however, they differ significantly in the couplings λ_1', λ_2' and λ_3 leading to different collider phenomenology.

3.2 Collider phenomenology

In this section, we discuss the possible signals of this model at HL-LHC and future e^+e^- colliders. As already mentioned, the invisible decay of the heavy Higgs into the dark matter candidate is a source of missing energy at colliders. Therefore, the direct production of heavy Higgs bosons and consequent decay of the Higgs to χ along with visible SM particles can give rise to distinct signatures for this scenario as opposed to the 2HDM like scenario. We investigate these possibilities and their prospects in the context of $\sqrt{s} = 14$ TeV LHC at the targeted

integrated luminosity of 3-4 ab^{-1} and of future e^+e^- colliders (ILC,CLIC) up to $\sqrt{s} = 3$ TeV and integrated luminosities of 5 ab^{-1}.

3.2.1 Prospects at LHC

The main processes contributing to neutral Higgs production at the LHC are gluon fusion (mediated by the top quark loop), vector boson fusion (VBF), associated Higgs production (Vh_i), $b\bar{b}h_i$, $t\bar{t}h_i$ [1]. For the charged Higgs pair, the possible production channels are H^+H^- and $W^\pm H^\mp$ [1]. At the LHC Run 3 at $\sqrt{s} = 14$ TeV, all possible Higgs production processes (including SM and BSM Higgses) are summarised in Table II.

In the presence of the heavy Higgs H decaying into two dark matter candidates, one gets invisible momentum in the final state and one can look into the following final states:

a) $1j$ (ISR)+missing E_T [25],

b) $2j$+ missing E_T [26] .

We estimate the significance for the mono-jet and VBF channels using the cuts from an existing cut-and-count analyses performed in [4] for $\sqrt{s} = 14$ TeV LHC, further details see [10]. For a) we achieve a cut efficiency for the signal in BP3 of about $\sim 18\%$ and we obtain a 0.111σ excess at 3ab^{-1} using gluon fusion production channel (at leading order (LO)). For b) we get a signal efficiency of 4.5% for BP3 and a signal significance of about $\sim 0.2\ \sigma$ at 3 ab^{-1}. Therefore, we observe that due to the small invisible branching ratio and heavy Higgs masses ~ 820 GeV (and hence small production cross section) in BP3, the final states will be inaccessible at the upcoming HL-LHC run.

3.2.2 Prospects at a high-energy e^-e^+ Linear Collider (ILC, CLIC)

The cleaner environment and lower background along the beam line compared to hadron colliders make the electron-positron linear colliders an attractive choice for precision studies of new physics.

The International Linear Collider (ILC) [27] , is a proposed e^+e^- linear collider design with simultaneously polarized $e^\pm$ beams and several stages of center-of-mass energies, i.e. at the SM-like Higgs threshold ($\sqrt{s} = 250$ GeV), at the top threshold ($\sqrt{s} = 350$ GeV) and at about $\sqrt{s} = 500$ GeV up to $\sqrt{s} = 1$ TeV with a maximum target integrated luminosity of $\mathcal{L} = 500$ fb^{-1}. The othe proposed high-energy e^+e^- linear collider design is CLIC [28,29] with an energy upgrade up to $\sqrt{s} = 1.5, 3$ TeV and at least a polarized e^-beam. An overview of the physics potential at future high-energy linear colliders is given in [30]. ILC (CLIC) gain advantage over the LHC in the possibility of exploiting the polarisation of the beams crucial both at the high energy stages but also already at the first stage of $\sqrt{s} = 250$ GeV [31, 32]. Although the invisible decay in BP3 is $H \to \chi\bar{\chi} \simeq 4.8\%$ and only a low production cross section times branching ratio is predicted, we observe that the $2b$+ missing E_T channel is observable with a $= 3.99\sigma$ significance at an integrated luminosity of $\mathcal{L} = 5$ ab^{-1}.

4 Conclusions and Outlook

We have studied dark matter phenomenology in a Two Higgs Doublet model with a complex scalar singlet where the scalar singlet doesn't obtain a vacuum expectation value. Benchmark scenarios consistent with all current experimental and cosmological constraints have been worked out. Particular stringent bounds on the available parameter range for the couplings are set by bounds from the direct detection. Due to very small rates of the heavy Higgs production,

Table 1: Relevant parameters of the benchmark points used for the study [10].

Parameters	BP1	BP2	BP3
λ_1	0.23	0.1	0.23
λ_2	0.25	0.26	0.26
λ_3	0.39	0.10	0.2
λ_4	-0.17	-0.10	-0.14
λ_5	0.001	0.10	0.10
$m_{12}^2 (\text{GeV}^2)$	-1.0×10^5	-1.0×10^5	-1.0×10^5
λ_1''	0.1	0.1	0.1
λ_3''	0.1	0.1	0.1
λ_1'	0.042	0.04	2.0
λ_2'	0.042	0.001	0.01
λ_4'	0.1	0.1	0.1
λ_5'	0.1	0.1	0.1
$\tan\beta$	4.9	6.5	6.5
m_h (GeV)	125.09	125.09	125.09
m_H (GeV)	724.4	816.4	821.7
m_A (GeV)	724.4	812.6	817.9
$m_{H^\pm}$ (GeV)	816.3	816.3	822.2
m_χ (GeV)	338.0	76.7	323.6
Ωh^2	0.058	0.119	0.05
$\sigma_p^{SI} \times 10^{10}$ (pb)	0.76	0.052	2.9
$\sigma_n^{SI} \times 10^{10}$ (pb)	0.78	0.054	3.1

Table 2: The leading order (LO) cross section (in fb), further details see [10].

| Processes	Cross section (in fb) at $\sqrt{s} = 14$ TeV		
	BP1	BP2	BP3
h (ggF)	29.3×10^3	29.3×10^3	29.3×10^3
H	22.61	5.238	6.632
A	35	8.58	10.8
hjj (VBF)	1.296×10^3	1.265×10^3	1.25×10^3
Hjj	1.843	1.845	0.56
Ajj	2.885	2.88	40.91
Wh	1.148×10^3	1.133	1.134 pb
WH	1.195×10^{-3}	1.11e-03	1.199×10^{-3}
WA	4.3×10^{-4}	5.892e-04	5.734×10^{-4}
Zh	880.8	677.2	697.9
ZH	0.93	0.2783	0.3408
ZA	3.999	1.413	1.689
bbh	2534	2541	2541 pb
bbH	21.52	17.92	17.92 fb
bbA	23.39	18.9	19.04fb
$t\bar{t}h$	478.3	477.1	477.9
$t\bar{t}H$	0.1988	0.06571	0.7891
$t\bar{t}A$	0.2552	0.08036	0.09826
H^+H^-	0.06603	0.03033	0.03416
$W^\pm H^\mp$	102.4	3.453	4.145
$\chi\bar{\chi} + 1j$	0.006356	0.0681	0.8819
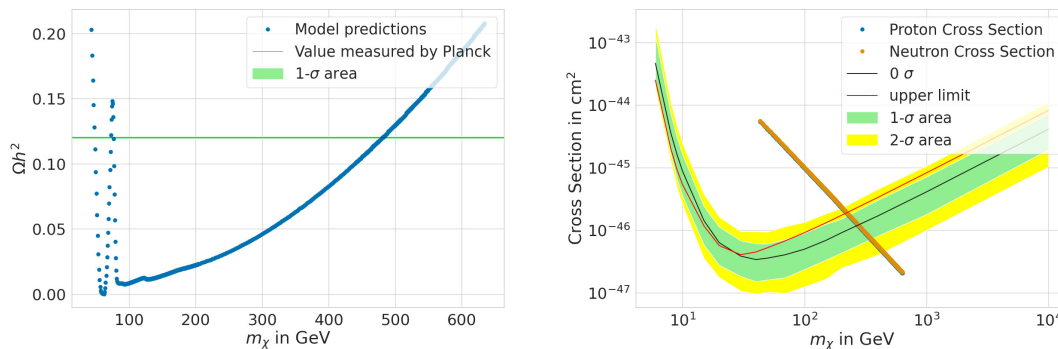
Figure 1: Relic density and direct detection cross-section predicted by the model depending on the DM mass m_χ [10]. The parameter m_S^2 has been varied in the range from 100-400000 GeV^2 and fixed $\tan\beta = 5$. The other parameters are chosen as in benchmark scenario BP1, see Table I.

the dark matter candidates will probably not be detectable via monojet or di-jet studies even at the HL-LHC. However, at a high-energy linear collider with polarized beams and precise initial energy, such a dark matter scenario is expected to be detectable. In addition, the option of direct dark matter pair production plus an ISR-photon is still under studies and offers another promising phenomenology. Further studies on exploring the mixing angles in the Higgs sector to shed light on the dark matter behaviour is still ongoing as well.

Acknowledgments

References

[1] G. C. Branco, P. M. Ferreira, L. Lavoura, M. N. Rebelo, M. Sher and J. P. Silva, *Theory and phenomenology of two-Higgs-doublet models*, Phys. Rep. **516**, 1 (2012), doi:10.1016/j.physrep.2012.02.002.

[2] B. Grzadkowski and P. Osland, *Tempered two-Higgs-doublet model*, Phys. Rev. D **82**, 125026 (2010), doi:10.1103/PhysRevD.82.125026.

[3] A. Drozd, B. Grzadkowski, J. F. Gunion and Y. Jiang, *Extending two-Higgs-doublet models by a singlet scalar field — The case for dark matter*, J. High Energy Phys. **11**, 105 (2014), doi:10.1007/JHEP11(2014)105.

[4] A. Dey, J. Lahiri and B. Mukhopadhyaya, *LHC signals of a heavy doublet Higgs as dark matter portal: cut-based approach and improvement with gradient boosting and neural networks*, J. High Energy Phys. **09**, 004 (2019), doi:10.1007/JHEP09(2019)004.

[5] S. Baum and N. R. Shah, *Two Higgs doublets and a complex singlet: disentangling the decay topologies and associated phenomenology*, J. High Energy Phys. **12**, 044 (2018), doi:10.1007/JHEP12(2018)044.

[6] G. C. Dorsch, S. J. Huber, T. Konstandin and J. M. No, *A second Higgs doublet in the early universe: baryogenesis and gravitational waves*, J. Cosmol. Astropart. Phys. **2017**, 052 (2017), doi:10.1088/1475-7516/2017/05/052.

[7] T. Biekötter and M. O. Olea-Romacho, *Reconciling Higgs physics and pseudo-Nambu-Goldstone dark matter in the S2HDM using a genetic algorithm*, J. High Energy Phys. **10**, 215 (2021), doi:10.1007/JHEP10(2021)215.

[8] V. Barger, P. Langacker, M. McCaskey, M. Ramsey-Musolf and G. Shaughnessy, *Complex singlet extension of the standard model*, Phys. Rev. D **79**, 015018 (2009), doi:10.1103/PhysRevD.79.015018.

[9] P. Bechtle, S. Heinemeyer, O. Stål, T. Stefaniak and G. Weiglein, *Probing the Standard Model with Higgs signal rates from the Tevatron, the LHC and a future ILC*, J. High Energy Phys. **11**, 039 (2014), doi:10.1007/JHEP11(2014)039.

[10] J. Dutta, G. Moortgat-Pick and M. Schreiber, *Phenomenology of the Dark Matter sector in the 2HDM extended with Complex Scalar Singlet*, (arXiv preprint) doi:10.48550/arXiv.2203.05509.

[11] K. G. Klimenko, *On necessary and sufficient conditions for some higgs potentials to be bounded from below*, Theor. Math. Phys. **62** (1985), 58.

[12] K. Kannike, *Vacuum stability conditions from copositivity criteria*, Eur. Phys. J. C **72**, 2093 (2012), doi:10.1140/epjc/s10052-012-2093-z.

[13] P. Bechtle, S. Heinemeyer, T. Klingl, T. Stefaniak, G. Weiglein and J. Wittbrodt, *HiggsSignals-2: probing new physics with precision Higgs measurements in the LHC 13 TeV era*, Eur. Phys. J. C **81**, 145 (2021), doi:10.1140/epjc/s10052-021-08942-y.

[14] P. Bechtle, D. Dercks, S. Heinemeyer, T. Klingl, T. Stefaniak, G. Weiglein and J. Wittbrodt, *HiggsBounds-5: testing Higgs sectors in the LHC 13 TeV Era*, Eur. Phys. J. C **80**, 1211 (2020), doi:10.1140/epjc/s10052-020-08557-9.

[15] W. Porod and F. Staub, *SPheno 3.1: extensions including flavour, CP-phases and models beyond the MSSM*, Comput. Phys. Commun. **183**, 2458 (2012), doi:10.1016/j.cpc.2012.05.021.

[16] N. Aghanim et al., *<i>Planck</i>2018 results*, Astron. Astrophys. **641**, A6 (2020), doi:10.1051/0004-6361/201833910.

[17] E. Aprile, *Dark matter search results from a one ton-year exposure of XENON1T*, Phys. Rev. Lett. **121**, 111302 (2018), doi:10.1103/PhysRevLett.121.111302.

[18] M. Ackermann, *Constraining dark matter models from a combined analysis of Milky Way satellites with the Fermi Large Area Telescope*, Phys. Rev. Lett. **107**, 241302 (2011), doi:10.1103/PhysRevLett.107.241302.

[19] G. Bélanger, A. Mjallal and A. Pukhov, *Recasting direct detection limits within micrOMEGAs and implication for non-standard dark matter scenarios*, Eur. Phys. J. C **81**, 239 (2021), doi:10.1140/epjc/s10052-021-09012-z.

[20] F. Staub, *SARAH 4: A tool for (not only SUSY) model builders*, Comput. Phys. Commun. **185**, 1773 (2014), doi:10.1016/j.cpc.2014.02.018.

[21] J. Alwall et al., *The automated computation of tree-level and next-to-leading order differential cross sections, and their matching to parton shower simulations*, J. High Energy Phys. **07**, 079 (2014), doi:10.1007/JHEP07(2014)079.

[22] C. Bierlich et al., *A comprehensive guide to the physics and usage of PYTHIA 8.3*, SciPost Phys. Codebases 8 (2022), doi:10.21468/SciPostPhysCodeb.8.

[23] J. de Favereau et al., *DELPHES 3: a modular framework for fast simulation of a generic collider experiment*, J. High Energy Phys. **02**, 057 (2014), doi:10.1007/JHEP02(2014)057.

[24] J. Y. Araz, B. Fuks and G. Polykratis, *Simplified fast detector simulation in MadAnalysis 5*, Eur. Phys. J. C **81**, 329 (2021), doi:10.1140/epjc/s10052-021-09052-5.

[25] ATLAS:2021kxv G. Aad *et al.* [ATLAS],

The ATLAS Collaboration , *Search for new phenomena in events with an energetic jet and missing transverse momentum in pp collisions at $\sqrt{s}$ =13 TeV with the ATLAS detector*, Phys. Rev. D **103**, 112006 (2021), doi:10.1103/PhysRevD.103.112006.

[26] The ATLAS Collaboration, *Search for invisible Higgs boson decays with vector boson fusion signatures with the ATLAS detector using an integrated luminosity of 139 fb^{-1}* (2020), https://cds.cern.ch/record/2715447?ln=en.

[27] C. Adolphsen et al., *The International linear collider technical design report - Volume 3.II: Accelerator baseline design*, (arXiv preprint) doi:10.48550/arXiv.1306.6328.

[28] P. N. Burrows et al., *The Compact Linear Collider (CLIC) - 2018 summary report* (2018), doi:10.23731/CYRM-2018-002.

[29] A. Robson and P. Roloff, *Updated CLIC luminosity staging baseline and Higgs coupling prospects*, arXiv:1812.01644.

[30] G. Moortgat-Pick et al., *Physics at the e^+e^- linear collider*, Eur. Phys. J. C **75**, 371 (2015), doi:10.1140/epjc/s10052-015-3511-9.

[31] G. Moortgat-Pick et al., *Polarized positrons and electrons at the linear collider*, Phys. Rep. **460**, 131 (2008), doi:10.1016/j.physrep.2007.12.003.

[32] K. Fujii et al., *The role of positron polarization for the inital 250 GeV stage of the International Linear Collider*, (arXiv preprint) doi:10.48550/arXiv.1801.02840.